University of Dundee

Selective Metallization of 3D Printable Thermoplastic Polyurethanes

Ryspayeva, Assel; Jones, Thomas D. A.; Khan, Sadeque Reza; Nekouie Esfahani, Mohammadreza; Shuttleworth, Matthew P.; Harris, Russell A.; Kay, Robert W.; Desmulliez, Marc Phillipe Yves; Marques-Hueso, Jose

Published in:
IEEE Access

DOI:
10.1109/access.2019.2931594

Publication date:
2019

Document Version
Publisher's PDF, also known as Version of record

Link to publication in Discovery Research Portal

Citation for published version (APA):
Ryspayeva, A., Jones, T. D. A., Khan, S. R., Nekouie Esfahani, M., Shuttleworth, M. P., Harris, R. A., ... Marques-Hueso, J. (2019). Selective Metallization of 3D Printable Thermoplastic Polyurethanes. *IEEE Access*, *7*(2019). https://doi.org/10.1109/access.2019.2931594

General rights
Copyright and moral rights for the publications made accessible in Discovery Research Portal are retained by the authors and/or other copyright owners and it is a condition of accessing publications that users recognise and abide by the legal requirements associated with these rights.

- Users may download and print one copy of any publication from Discovery Research Portal for the purpose of private study or research.
- You may not further distribute the material or use it for any profit-making activity or commercial gain.
- You may freely distribute the URL identifying the publication in the public portal.

Take down policy
If you believe that this document breaches copyright please contact us providing details, and we will remove access to the work immediately and investigate your claim.

This article has been accepted for publication in a future issue of this journal, but has not been fully edited. Content may change prior to final publication. Citation information: DOI 10.1109/ACCESS.2019.2931594, IEEE Access

Selective Metallization of 3D Printable Thermoplastic Polyurethanes

Assel Ryspayeva, Thomas D. A. Jones, Sadeque Reza Khan, Mohammadreza Nekouie Esfahani, Matthew P. Shuttleworth, Russell A. Harris, Robert W. Kay, Marc P.Y. Desmulliez, *Senior Member IEEE*, and Jose Marques-Hueso

***Abstract*—This article presents a selective metallization method for the newly developed 3D printable thermoplastic polyurethane elastomers (TPU): FilaFlex®, SemiFlex™, PolyFlex™ and NinjaFlex®. Silver nanoparticles were fabricated *in-situ* by photo-reduction on the surface of TPUs and acted as catalysts for copper ion adsorption. This method demonstrates the successful fabrication of copper patterns on flexible TPU filaments. Furthermore, Polyflex™ and acrylonitrile butadiene styrene (ABS) filaments printed in the same part have been used to enable selective electroless plating directly on Polyflex™ material. Electroless copper deposited onto Polyflex™ has a sheet resistance of (139.4 ± 7.2) mΩ/□ and a copper conductivity of (1.1 ± 0.1) × 10^7 S/m that is comparable to bulk copper. Copper-plated Polyflex™ interconnects were fabricated as a proof of concept demonstrators.**

***Index Terms*—Thermoplastic polyurethane elastomers (TPU), fused filament fabrication (FFF), 3D printing, additive manufacturing (AM), hybrid-AM, silver nanoparticles (Ag NPs), electroless copper plating, FilaFlex®, SemiFlex™, PolyFlex™, NinjaFlex®.**

I. Introduction

DIGITALLY printed electronics using additive manufacturing (AM) has been steadily developing over the last three decades towards the manufacture of electronics components, devices and systems [1], [2]. AM such as 3D printing does not require high vacuum, high voltage deposition processes and multi-stage photolithography to produce conformable electronics [3], [4]. With the development of flexible electronics, metallized polymer films have gained an increased interest from the microelectronic packaging, computer technology and biomedical engineering community [5], [6]. Whilst a number of printing techniques, including ink-jet [7] and screen printing [8], have been adapted to print interconnects and circuitry on flexible substrates, fused filament fabrication (FFF) is currently one of the most commonly applied methods for printing plastic parts such as flexible polymeric substrates [4]. FFF printing works by the controlled extrusion of thermoplastic filaments onto a build platform using a layer-by-layer motion [9]. Although FFF is an attractive, simple and affordable manufacturing method to produce plastic parts and structures at relatively high speed [10], it is mostly limited to a certain number of thermoplastic filaments such as polycarbonate (PC), acrylonitrile butadiene styrene (ABS) and polylactic acid (PLA) [4], [9]. Nevertheless, new materials with superior flexible properties are constantly being researched, which include thermoplastic polyurethane elastomers (TPU). TPUs are multi-phase block copolymer that consists of rigid hard segments, diisocyanate and short chain extenders, and rubbery soft segments, commonly polyester or polyether-based, which are linked by hydrogen bonds [11]. These filaments mainly consist of polyurethane and additives to aid the printing process. Polyurethanes are attractive materials for flexible and stretchable electronics due to their outstanding elongation capacity, chemical resistance, thermal stability and versatility in applications [12]. Due to its wide mechanical and chemical properties, polyurethane finds applications in rigid and flexible substrates, adhesives, flame retardants, automobiles and biomedical applications [12]. These new TPUs still have to be tested for performance and behaviour during the printing process [13].

Whilst thermoplastic conductive filaments are continuously being developed for FFF printers [14], the electrical conductivity of these thermoplastic composite filaments remain generally low compared to their bulk metal counterparts [15]. In the pursuit of achieving 3D printing of multifunctional materials, hybrid-AM has therefore become one of the approaches to introduce metal parts on plastics by applying post-processing techniques [16], [17]. These include electroless plating and electroplating of 3D printed parts produced by stereolithography, laser sintering and FFF printers [18], [19]. Whilst electroplating requires a deposition of an additional metal layer on non-conductive surfaces, electroless plating allows metallization of 3D geometries with simpler equipment, reducing costs and increasing throughput [3], [20]. Therefore, post-processing of the TPUs may open new opportunities to create a bespoke circuitry and

This work is financially supported by the Engineering & Physical Sciences Research Council (EPSRC) under the grant Photobioform II (Grant Nos. EP/N018222/1 and EP/N018265/2).

A. Ryspayeva, S. Reza Khan, M. P.Y. Desmulliez, J. Marques-Hueso are with School of Engineering & Physical Sciences, Nature Inspired Manufacturing Centre (NIMC), Heriot Watt University, Edinburgh EH14 4AS, Scotland, UK. (e-mail: j.marques@hw.ac.uk).
T. D. A. Jones was formally with School of Engineering & Physical Sciences, NIMC, Heriot Watt University, Edinburgh EH14 4AS, Scotland, UK. He is now with School of Science and Engineering, The University of Dundee, Dundee, DD1 4HN, UK.
M. N. Esfahani, M. P. Shuttleworth, R. A. Harris, R. W. Kay are with Future Manufacturing Processes Research Group, School of Mechanical Engineering, University of Leeds, LS2 9JT, UK.

This work is licensed under a Creative Commons Attribution 4.0 License. For more information, see https://creativecommons.org/licenses/by/4.0/.

This article has been accepted for publication in a future issue of this journal, but has not been fully edited. Content may change prior to final publication. Citation information: DOI 10.1109/ACCESS.2019.2931594, IEEE Access

interconnects onto non-conductive flexible surfaces. Circuit structuring of the flexible polymers can be performed by using a laser direct structuring (LDS) [21] or laser-induced selective activation (LISA) [22]. However, these techniques frequently use expensive activators which include palladium [22], [23].

This article demonstrates the development of a direct and selective metallization method for TPU filaments and 3D printed TPU parts through surface treatment and electroless copper plating. This method does not require expensive vacuum processing, complex equipment and allows metallization of flexible substrates. Copper patterns could be formed directly on the 3D printed plastic structures with a good selectivity. Moreover, conductive segments could be realized on insulators, by printing multiple materials and plating them selectively with reduced number of steps. We study four recently developed TPU filaments: FilaFlex® (Recreus), SemiFlex™ (Ninjatek), PolyFlex™ (Polymaker) and NinjaFlex® (Ninjatek). The method involves the formation of photosensitive AgCl and photo-reduction of Ag ions to Ag nanoparticles (NPs) on the surface of the polyurethane material. These Ag NPs are shown to act as a catalysts for copper ion adsorption during the electroless copper plating [24]. Conductivity of the resulting metal films is comparable to values obtained in bulk metal.

II. Materials and Methods

In this study, four flexible 1.75 mm diameter TPU filaments were tested: FilaFlex® (Recreus), SemiFlex™ (Ninjatek), PolyFlex™ (Polymaker) and NinjaFlex® (Ninjatek). TPU filaments have outstanding elongation properties as shown in Table 1. A test scale for Shore hardness is A, which corresponds to a scale used for soft plastics in ISO 7619-1 [25].

TABLE I
MATERIAL PROPERTIES

	FilaFlex®	SemiFlex™	PolyFlex™	NinjaFlex®
Material	Polyether-poly-urethane	Poly-urethane	Poly-urethane	Poly-urethane
Shore hardness	82A	98A	95A	85A
Elongation (%)	665	600	330	660

Selective metallization method was applied directly to TPU filaments as well as to the 3D printed parts. Fig. 1 shows the process used to achieve a metal pattern on the TPU surface. 3D parts were also produced from the PolyFlex™ filament.

A. *Ag NPs Synthesis and Photo-patterning*

TPU filaments were cleaned in D.I. water using ultrasonic bath for 2 minutes. Samples were then immersed into a 15 M potassium hydroxide (KOH, Fisher Scientific, UK) solution at 50°C for 2 hours with stirring. After rinsing with D.I. water, samples were immersed into 0.1 M silver nitrate ($AgNO_3$, Fisher Scientific, UK) solution for 20 minutes at room temperature (RT). TPU samples were then rinsed with D.I. water and dried. Prior to the photo-patterning step, samples were immersed into a solution of 0.01 M potassium chloride (KCl, Fisher Scientific, UK) for 1 minute.

Photo-patterning was performed using a 3-minute LED exposure with a high-power (1 W) LED at 460 nm having a light intensity of 12 W/cm^2. A chromium on glass mask was used to selectively pattern TPU samples. The removal of the unexposed and unwanted Ag ions was performed through a wet etching with 18% ammonia solution (NH_3, Fisher Scientific, UK) for 3 minutes following by 5% sulfuric acid (H_2SO_4, Fisher Scientific, UK) for 1 minute with a D.I rinse between each etching step. The application of etchants to the entire substrate surface removes unprocessed Ag ions weakly bound to the substrate with little removal of the Ag metal [24] [26] and, therefore, allow successful selective electroless copper plating.

B. *Electroless Copper Plating*

Electroless copper solution was prepared by dissolving 6 g of copper sulfate (98%, Sigma Aldrich), 8 g of sodium hydroxide (98.5%, Acros Organics), and 28 g of potassium tartrate (99%, Fisher Scientific) into 200 ml of DI water. Before electroless plating, 12 mL of the concentrated solution was diluted with DI water in the ratio of 1:1 and 2 ml of formaldehyde (37 %, Acros Organics) was added. TPU samples were immersed into electroless copper bath and plated at 30°C for 20 minutes.

C. *Characterization*

Fourier-transform infrared spectroscopy (FTIR) was obtained using a Perkin-Elmer Spectrum 100 FT-IR spectrometer operated in attenuated total reflection mode. Optical images were obtained with LEICA CTR 6500 microscope. Scanning electron microscopy (SEM) was performed with a Quanta 3-D FEG. Ag NPs and copper grains average sizes (diameters) were measured using the Fiji (based on ImageJ) open source image processing software. Resistance was measured with SIGNATONE S-1160 two-point probe station. Sheet resistance measurement was performed on metallized PolyFlex™ TPU square samples (20 mm × 20 mm) using a Jandel Model RM3000 four-point probe station (England). The conductivity was calculated as the inverse of the resistivity, ρ which was found from the product of sheet resistance, R_s and the copper thickness, t:

$$\rho = R_s \times t \quad (1)$$

Copper thickness was measured using Dektak^3 Stylus profilometer. The quality of the metal plating adhesion was tested using the IPC-TM-650 scotch-tape test on the square samples [27]. Pressure sensitive tape was pressed across the metallized PolyFlex™ TPU square samples of 20 mm × 20 mm size. The tape was pulled rapidly and visually examined for any material removal from the specimen. The test was performed three times on three different samples. The percentage of the removed copper from the PolyFlex™ substrate was evaluated using digital image processing. Digital images of the scotch-tape with the removed copper were converted to 8-bit type, and segmented by thresholding to locate the regions of the

This work is licensed under a Creative Commons Attribution 4.0 License. For more information, see https://creativecommons.org/licenses/by/4.0/.

This article has been accepted for publication in a future issue of this journal, but has not been fully edited. Content may change prior to final publication. Citation information: DOI 10.1109/ACCESS.2019.2931594, IEEE Access

removed copper using Fiji. Black and white (BW) images where evaluated in MATLAB (The MathWorks Inc.) by counting all the dark pixels and calculating the percentages of the removed copper.

D. Printing of 3D Parts

Production of 3D parts was performed using a MakerBot Replicator 2X (MakerBot Industries, LLC, Brooklyn, NY). The building platform was covered with a painter's tape (Scotch Blue 2093EL tape, 3M) for adhesion. The thickness of the individual layer was set to 0.2 mm with 100 % infill. A PolyFlex™ substrate was printed with an extrusion temperature of 230 °C and a bed temperature of 60 °C.

3D structure of a PolyFlex™ part on ABS substrate was printed with an extrusion temperature of 230 °C and 100 °C bed temperature.

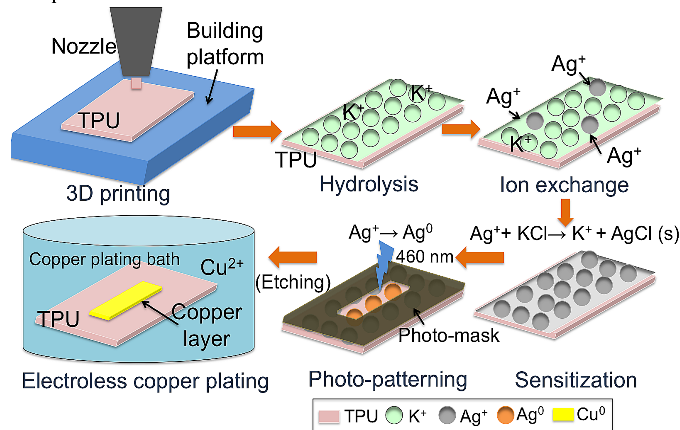

Fig. 1. Schematic steps of selective metallization of TPU material. Clockwise: 3D printing of the required structure, hydrolysis, ion exchange, sensitization, photo-patterning and electroless copper plating.

III. RESULTS AND DISCUSSIONS

A. Surface treatment

The general chemical structure of the polyurethane is shown in Fig.2a, which consists of the hard and soft segments linked through the –NH-(C=O)-O- urethane group [28]. The surface of the TPU filaments is expected to be modified by the highly alkaline KOH solution, as demonstrated in [24], [26] by FTIR measurements of polymer substrates. For this reason, FTIR scans have been applied here for the four TPU filaments at different stages of processing, as shown in Fig. 2. Spectra of the TPU materials were taken for untreated samples, samples treated with KOH and samples treated with $AgNO_3$. The exact chemical composition of the filament is unknown, however, it is known that Filaflex is a polyether-polyurethane [29]. Since the FTIR spectra in Fig. 2 d-f are similar to the Filaflex spectrum in Fig. 2c, it is presumed that TPU filaments exhibit polyether-based polyurethanes characteristics. Polyether-polyurethanes are highly resistant to hydrolysis and bacteria and, therefore, are desirable for medical applications [30]. However, under severe conditions such as strong alkali treatment, polyether polyurethane can undergo hydrolysis, which occurs at urethane linkage [31], [32]. Urethane is a derivative of the amide and, therefore, undergoes the same hydrolysis mechanism as for amides, Fig.2b [33]. Samples treated with silver nitrate have similar peaks as samples after hydrolysis since potassium ions exchanged with silver ions (Fig. 2b) do not lead to changes in FTIR spectra [24].

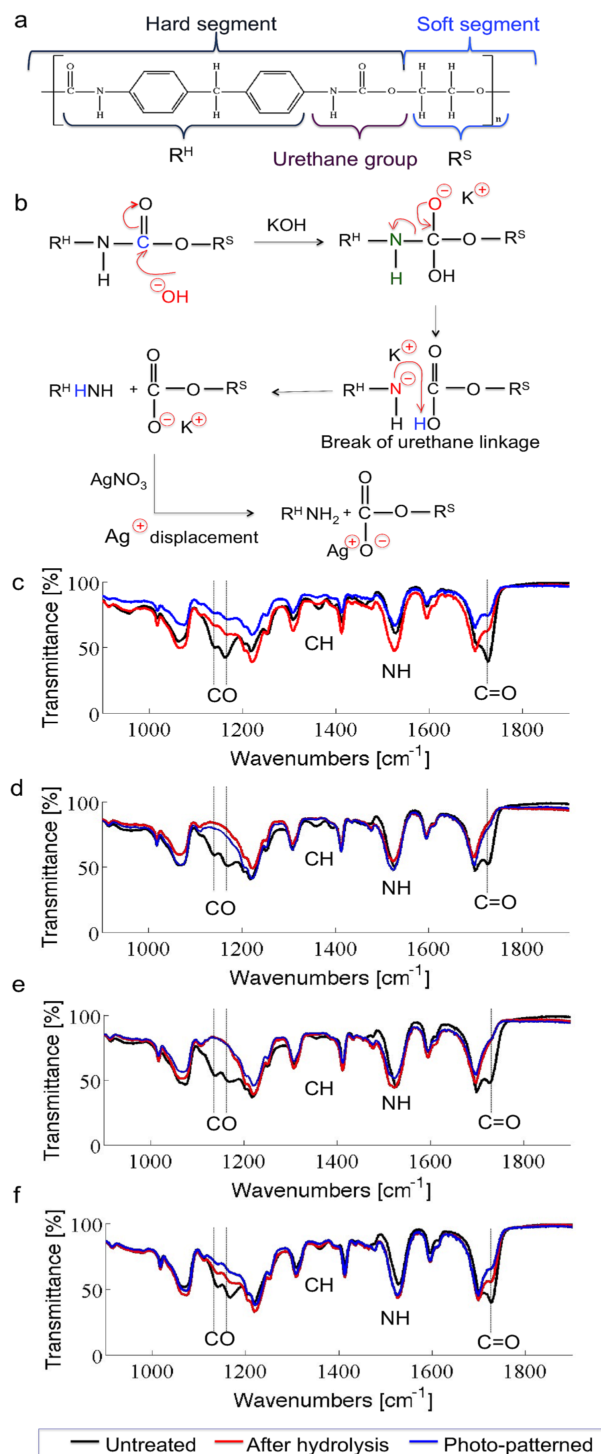

Fig. 2. a) A schematic of a polyurethane structure that consists of hard and soft segments, (b) a schematic for hydrolysis and ion exchange mechanism, where potassium ions are displaced with silver ions. R^H and R^S stand for functional groups of the hard and soft segments of the polyurethane, respectively. FTIR spectra measured for filaments: c) FilaFlex®, d) SemiFlex™, e) PolyFlex™ and f) NinjaFlex® at different process stages.

The absorption band at around 1725 cm^{-1} is due to a stretching vibration of amide band (-C=O) of urethane [34]. Secondary

This work is licensed under a Creative Commons Attribution 4.0 License. For more information, see https://creativecommons.org/licenses/by/4.0/.

This article has been accepted for publication in a future issue of this journal, but has not been fully edited. Content may change prior to final publication. Citation information: DOI 10.1109/ACCESS.2019.2931594, IEEE Access

urethanes absorb strongly at 1525 cm^{-1} due to –CNH- group vibration [35]. The vibration band at 1700 cm^{-1} is attributed to hydrogen bond between N-H and C=O groups in the hard segment [36], [37]. Esters, ethers and carboxylic groups absorb strongly in the range between 1300 cm^{-1} and 1000 cm^{-1} due to C-O stretching vibrations [34]. The peak at 1725 cm^{-1} (amide band) that is present in the untreated samples is attenuated for all treated samples, indicating that the urethane linkage is broken due to hydrolysis [30], [38]. Moreover, peaks at 1162 cm^{-1} (C-O) and 1139 cm^{-1} (C-O) are also attenuated, which indicates that hydrolysis may also take place in the various functional groups of the soft segments (e.g hydrolysis of esters) in the polyurethane structure [32], [38]. The complete cleavage of the above mentioned peaks is observed in SemiFlex™ and PolyFlex™ (Fig. 2 d, e), which suggests that these TPU filaments are more susceptible to alkaline attack.

Prior to light exposure, a sensitization step was utilized to accelerate formation of Ag NPs during the photo-reduction step. Silver treated filaments were immersed into solution of 0.01 M KCl in ethanol:water (3:1) to form highly photosensitive AgCl. This sensitization step was successfully demonstrated and discussed in previously published work [24], [26].

The distribution of NPs across a surface influences the quality of the further processing by electroless copper [24], [26]. The NP dispersion is a figure of merit that can characterize NP treatment performance and can be evaluated from SEM images of Ag treated surfaces [26]. Fig. 3 shows SEM images of the photo-reduced Ag NPs on TPU surfaces with the insets displaying the histogram plots of Ag NPs size distribution. The average size of Ag NPs reduced on FilaFlex™ (label a Fig. 3) is 17 nm ± 5 nm. Ag NPs are monodisperse with a polydispersity index of 0.29, covering the polymer surface uniformly.

The average sizes of Ag NPs formed on Semiflex™, PolyFlex™ and NinjaFlex® filaments (label b, c, d in Fig. 3) are 58 nm ± 27 nm, 68 nm ± 41 nm and 38 nm ± 20 nm, respectively. Ag NPs appear spherical in shape forming agglomerates. The nanoparticles have a broad size distribution with polydispersity indices of 0.47, 0.6 and 0.52, respectively. Ag NPs photo-reduced on PolyFlex™ are more densely packed as compared to nanoparticles formed on Semiflex™ and NinjaFlex®. High nanoparticle densities provide higher surface coverage and therefore, are favorable for uniform and successful electroless copper deposition [26].

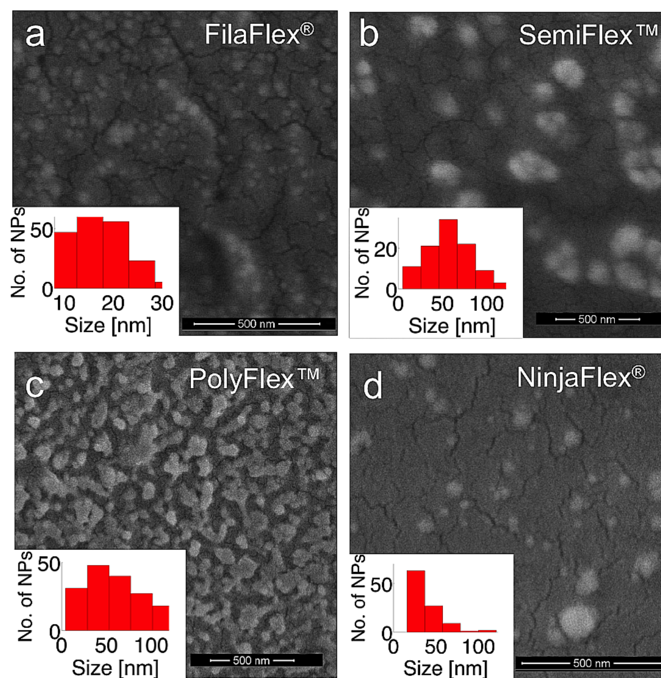

Fig. 3. SEM micrographs showing photo-reduced Ag NPs on TPU filaments: a) FilaFlex®, b) SemiFlex™, c) PolyFlex™, d) NinjaFlex®. The insets show size distribution of Ag NPs.

Fig. 4 shows images of the photo-reduced patterns produced on TPU filaments where silver ions were successfully reduced on all four TPU filaments. The photo-reduced Ag NPs appear yellow in color in FilaFlex®, Semiflex™and NinjaFlex® samples. The pattern on PolyFlex™ shows a brown color which indicates the formation of a high concentration of Ag NPs [39], [40]. This could be due to a more successful hydrolysis, which resulted in a large Ag ions density. Therefore, the pattern on PolyFlex™ is more well defined compared to the patterns on others filaments.

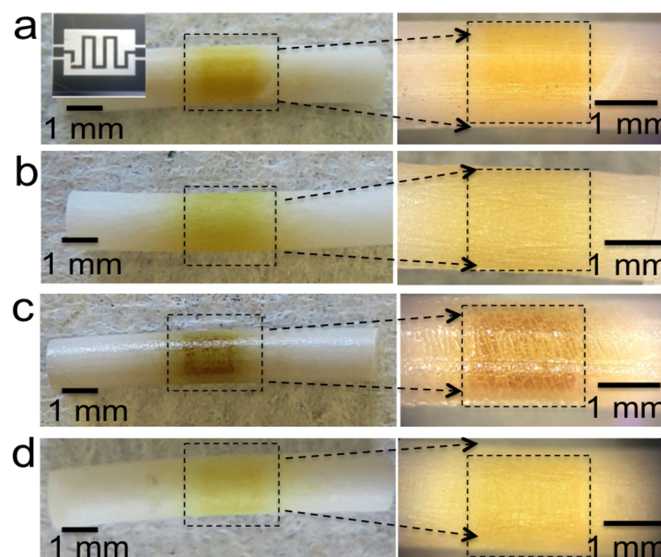

Fig. 4. Images of TPU filaments after photo-reduction: a) FilaFlex®, b) SemiFlex™, c) PolyFlex™ and d) NinjaFlex®. The inset shows the photo-mask used during the LED exposure.

This work is licensed under a Creative Commons Attribution 4.0 License. For more information, see https://creativecommons.org/licenses/by/4.0/.

This article has been accepted for publication in a future issue of this journal, but has not been fully edited. Content may change prior to final publication. Citation information: DOI 10.1109/ACCESS.2019.2931594, IEEE Access

B. Electroless Copper Metallization of TPU Filaments

After the photo-reduction step, the TPU filaments were immersed into electroless copper bath. Ag NPs act as catalytic centers for copper ions adsorption [41]. Electron transfer to the adsorbed copper ions on the silver seeds results in the deposition of copper metal on the catalytic substrate. Equation (2) shows an overall reaction for the electroless copper deposition with formaldehyde (HCHO) as a reducing agent [42], [43]:

$$Cu^{2+} + 2HCHO + 4OH^{-} \rightarrow Cu + 2HCOO^{-} + 2H_2O + H_2 \quad (2)$$

The deposited copper metal then serves as a seed layer for subsequent copper ion adsorption and process repeats [44].

Fig. 5 shows SEM images of copper layers deposited onto TPU filaments and insets depicting the average grain size distribution. Copper layers have a granular structure covering TPU surfaces uniformly. The average sizes of the copper grains are 0.6 µm ± 0.4 µm, 0.3 µm ± 0.1 µm, 0.2 µm ± 0.1 µm, 0.4 µm ± 0.1 µm for FilaFlex™, SemiFlex™, PolyFlex™ and NinjaFlex®, respectively. Copper layers on all samples are shown to have voids between the grains. These voids may form due to hydrogen release during the simultaneous reduction of copper and hydrogen [45], which results in trapping of hydrogen gas bubbles in copper grains forming voids [46]. Copper layer formed on PolyFlex™ has small grains that packed more densely than other copper depositions. Its higher density stems from the high amount of Ag NPs in the PolyFlex™ polymer, see Fig. 3, which creates more sites for copper ion adsorption.

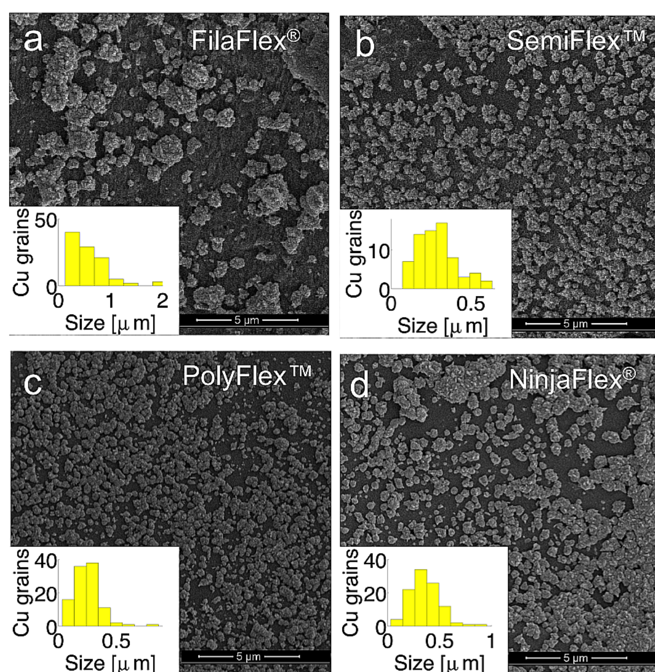

Fig. 5. SEM micrographs showing electroless copper layer on TPU filaments: a) FilaFlex®, b) SemiFlex™, c) PolyFlex™, d) NinjaFlex®. The insets show size distribution of Cu grains.

Fig. 6 shows images of TPU filaments after electroless copper plating. The patterns on FilaFlex®, SemiFlex™ and NinjaFlex® filaments are less defined than on the PolyFlex™ filament. The copper pattern on PolyFlex™ resulted in a better-defined structure with a resistance of 34 ± 9 Ω, while the resistances of the metal layers on the other filaments ranged in the kΩ. Therefore, PolyFlex™ was the most suitable material choice for selective metallization of 3D printed parts, presented in the section C.

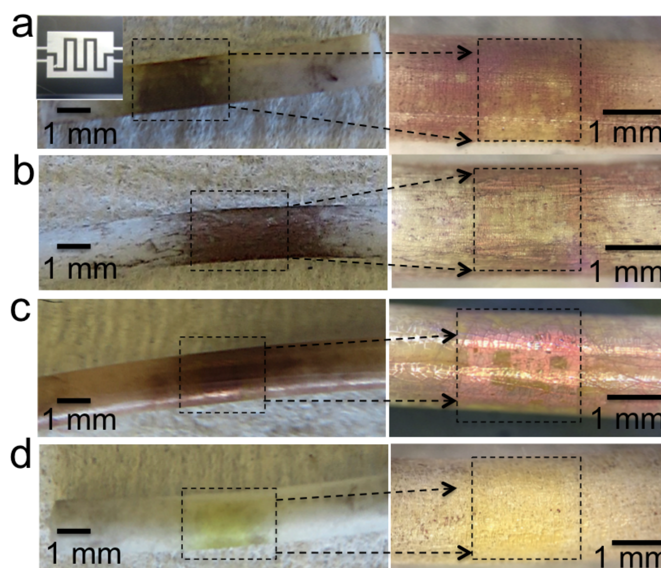

Fig. 6. Images of TPU filaments after electroless copper plating: a) FilaFlex®, b) SemiFlex™, c) PolyFlex™ and d) NinjaFlex®. The inset shows photo-mask used during the LED exposure.

C. Selective Metallization of 3D Printed Parts

A sheet resistance of 139.4 ± 7.2 mΩ/□ was measured for the metallized 3D printed PolyFlex™ square samples, which is in agreement with previously reported values [3], [47]. Copper conductivity is calculated as $(1.1 \pm 0.1) \times 10^{7}$ S/m for grown thickness (0.6 ± 0.1) µm, which is comparable to bulk copper values (5.9×10^{7} S/m). Fig. 7 a, b shows optical images of the metallized PolyFlex™ square sample after a scotch-tape test and a tape with the removed copper. Fig.7c shows a BW binary image of the tape image. The black color indicates the removed copper from the surface of the metallized Polyflex™. The average percentage of the copper removed by the tape for the three tested samples is 7.3% from the surface area of 20 mm × 20 mm.

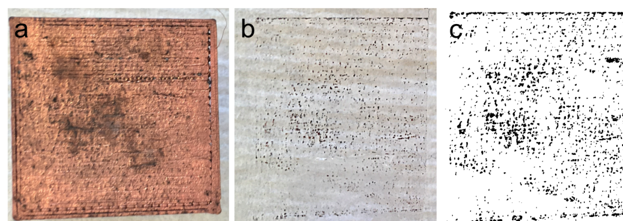

Fig. 7. Images of a) the metallized PolyFlex™ after IPC-TM-650 scotch-tape test, b) tape with the removed copper, c) conversion of the tape image to the BW binary image. Black color indicates the removed copper by the scotch-tape.

This work is licensed under a Creative Commons Attribution 4.0 License. For more information, see https://creativecommons.org/licenses/by/4.0/.

This article has been accepted for publication in a future issue of this journal, but has not been fully edited. Content may change prior to final publication. Citation information: DOI 10.1109/ACCESS.2019.2931594, IEEE Access

Fig. 8 shows images of the patterns fabricated on the 3D printed substrates made from the PolyFlex™ filament. The results show selective metallization where electroless copper plates on the catalyzed surfaces. Fig 8d shows a distribution of the measured feature sizes. The majority of the measured feature sizes are between 28 μm and 36.1 μm, whereas the actual feature size on the photo-mask is 28 μm. The smallest and largest sizes measured were 20 μm and 64 μm, respectively which highlights that some downsizing and enlarging of the feature size may occur.

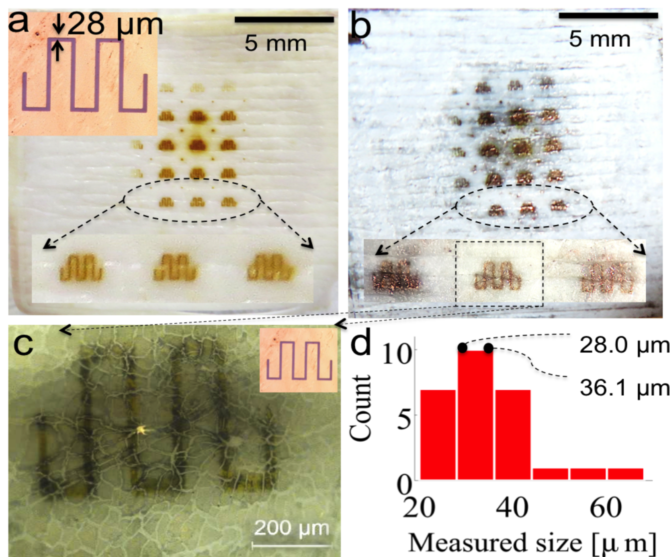

Fig. 8. Images of the 3D printed PolyFlex™ substrate with features: a) after photo-patterning and b) after electroless copper plating, c) a feature under the optical microscope; and d) a distribution of the measured pattern size. The insets show the photo-mask with the 28 μm feature size.

The metallization selectivity was further studied and Fig. 9 shows images of the photo-patterned and copper metallized features on the Polyflex™ substrate. Fig. 9 (d) shows the magnified copper patterns, in which a relatively well-defined boundary between the copper and the polymer is revealed. However, the resultant copper feature size (≈ 449.2 μm) has enlarged more than twice the size of the photo-mask feature (220 μm).

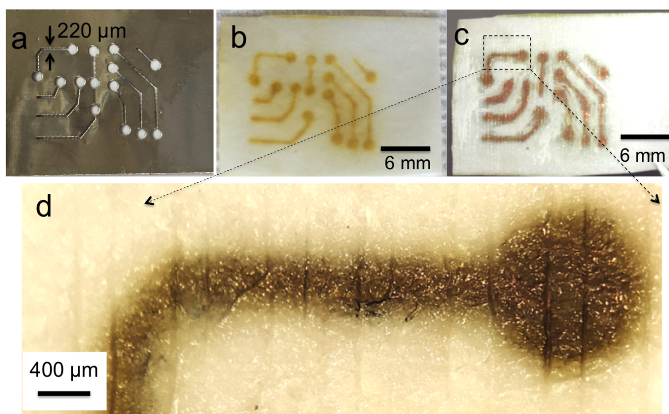

Fig. 9. Images of a) a laboratory-made photo-mask, b) PolyFlex™ substrate with features after photo-patterning and c) after electroless copper plating, d) a feature under the optical microscope.

Conductive segments could be realized on insulators, by printing multiple materials. As a demonstration, Fig. 10a shows images of the 3D printed PolyFlex™ pattern onto an ABS substrate after the LED exposure. ABS undergoes the same treatment as PolyFlex™, however, due to the lack of Ag ion exchange with ABS, the etching step to remove unwanted silver ions is not required. Therefore, by submerging the photoreduced Ag-Polyflex™-ABS 3D structure into the electroless copper bath, copper plated selectively on the PolyFlex™ part only with a resistance 5 ± 1 Ω, leaving ABS unaffected, Fig. 10b. Hence, plating could be performed selectively between the two polymer materials.

Fig. 10d shows PolyFlex™ pattern printed on the ABS, which is copper plated directly after silver nitrate treatment, but without a prior LED exposure. Therefore, it is possible to metallize PolyFlex™ on ABS directly in a more environmentally friendly process that negates harmful etchants and with fewer numbers of steps.

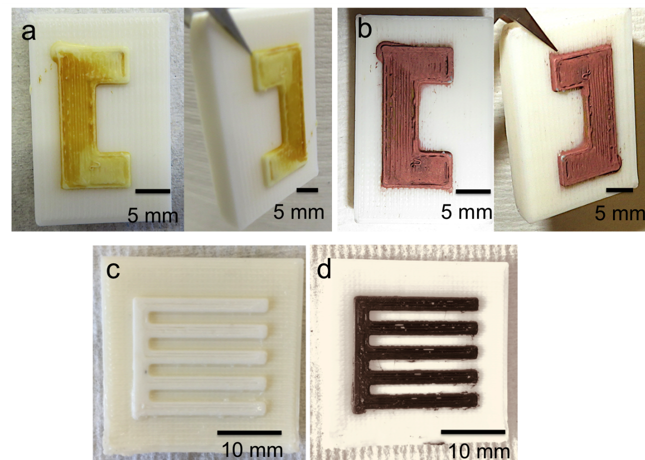

Fig. 10. Selective metallization of 3D printed structure of PolyFlex™ pattern printed on the ABS substrate: a) after LED exposure and b) after electroless copper plating. Images of PolyFlex™ pattern on ABS substrate plated without prior LED exposure c) initial sample and d) after electroless copper plating.

D. Copper-plated PolyFlex™ Interconnections

As a demonstration, copper-plated PolyFlex™ parts were adhered using a glue to a hand prototype, which was printed from PolyFlex™ filament, and acted as interconnections between a motor and a motor driving circuit (label a, b Fig. 11). The wires from the motor driving circuit were connected with the PolyFlex™ interconnects by scotch tape. Arduino Nano 3.0 (ATmega328) microcontroller is used to control the rotation of the DC motor (Q4SL2BQ280001), which is connected to a finger of the hand. The pulse width modulation (PWM) feature of the microcontroller is used to regulate the motor speed. Furthermore, a totem pole structure using PMF370XN N-channel MOSFET is adopted to control the bidirectional rotation of the DC motor. Therefore, when the motor rotates upwards it drives the finger in the same direction and, when the motor rotates downwards it will then drive the finger down. Fig. 11 c, d shows the movement of the finger in upward and downward directions as a result of the motor rotation. Therefore, with this demonstration, copper-plated

This work is licensed under a Creative Commons Attribution 4.0 License. For more information, see https://creativecommons.org/licenses/by/4.0/.

This article has been accepted for publication in a future issue of this journal, but has not been fully edited. Content may change prior to final publication. Citation information: DOI 10.1109/ACCESS.2019.2931594, IEEE Access

PolyFlex™ parts are proved to function as interconnections in the electronic circuit.

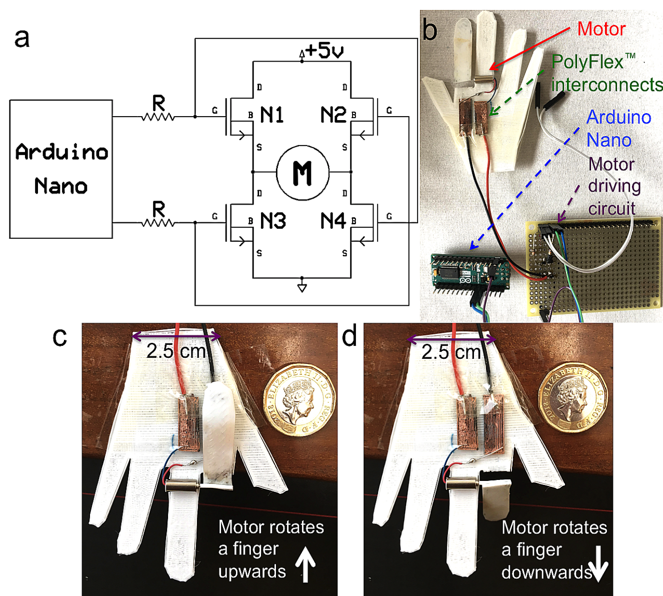

Fig. 11. A hand demonstrator with the copper-plated PolyFlex™ interconnects connecting a motor attached to a finger with a motor driver circuit: a) schematic of the motor driver circuit, b) a set-up of the printed hand with a motor connected through copper-plated PolyFlex™ interconnections, c) motor rotates a finger upwards, d) motor rotates a finger downwards.

IV. Conclusion

Four flexible TPU filaments were selectively metallized using a novel electroless copper metallization method. This method allows the fabrication of conductive patterns onto 3D printed flexible substrates. Furthermore, it is possible to fabricate conductive segments on non-conductive substrates by direct electroless plating of the 3D printed structure by submerging the whole structure at once. The electroless copper displayed a sheet resistance of (139.4 ± 7.2) mΩ/□ and a conductivity of $(1.1 \pm 0.1) \times 10^7$ S/m which is comparable to bulk values. This work could be further improved by obtaining better-defined patterns on the TPU substrates by applying photo-reduction at a shorter wavelength.

Acknowledgment

The authors would like to thank Mr. Mark Leonard, experimental officer at Heriot-Watt University for his assistance with the electrical and microscopic characterization facilities and Mr. Meshari Alsharari for his assistance with the FFF printer, Dr. Brian Hutton, a senior chemistry technician and Dr. Kristoffer Johansen for constructive discussions.

References

[1] O. F. Swenson and V. Marinov, “Laser Processing of Direct-Write Nano-Sized Materials,” in *Advances in Laser Materials Processing*, Elsevier, 2018, pp. 571–594.

[2] B. Grynol, “Disruptive manufacturing. The effects of 3D printing,” 2013.

[3] Y. Wang *et al.*, “Facile preparation of a high-quality copper layer on epoxy resin via electroless plating for applications in electromagnetic interference shielding,” *J. Mater. Chem. C*, vol. 5, no. 48, pp. 12769–12776, 2017.

[4] T. D. Ngo, A. Kashani, G. Imbalzano, K. T. Q. Nguyen, and D. Hui, “Additive manufacturing (3D printing): A review of materials, methods, applications and challenges,” *Compos. Part B Eng.*, vol. 143, pp. 172–196, 2018.

[5] J. H. Kim *et al.*, “Simple and cost-effective method of highly conductive and elastic carbon nanotube/polydimethylsiloxane composite for wearable electronics,” *Sci. Rep.*, vol. 8, no. 1, pp. 1–11, 2018.

[6] A. Ryspayeva *et al.*, “A rapid technique for the direct metallization of PDMS substrates for flexible and stretchable electronics applications,” *Microelectronic Engineering*, vol. 209. pp. 35–40, 2019.

[7] N. C. Raut and K. Al-Shamery, “Inkjet Printing Metals on Flexible Materials for Plastic and Paper Electronics,” *J. Mater. Chem. C*, vol. 6, no. 7, pp. 1618–1641, 2018.

[8] X. Cao *et al.*, “Screen Printing as a Scalable and Low-Cost Approach for Rigid and Flexible Thin-Film Transistors Using Separated Carbon Nanotubes,” *ACS Nano*, vol. 8, no. 12, pp. 12769–12776, Dec. 2014.

[9] X. Wang, M. Jiang, Z. Zhou, J. Gou, and D. Hui, “3D printing of polymer matrix composites: A review and prospective,” *Compos. Part B Eng.*, vol. 110, pp. 442–458, Feb. 2017.

[10] H. Bikas, P. Stavropoulos, and G. Chryssolouris, “Additive manufacturing methods and modeling approaches: A critical review,” *Int. J. Adv. Manuf. Technol.*, vol. 83, no. 1–4, pp. 389–405, 2016.

[11] D. J. Martin, A. F. Osman, Y. Andriani, and G. A. Edwards, “Thermoplastic polyurethane (TPU)-based polymer nanocomposites,” *Adv. Polym. Nanocomposites Types Appl.*, pp. 321–350, 2012.

[12] H. M. C. C. Somarathna, S. N. Raman, D. Mohotti, A. A. Mutalib, and K. H. Badri, “The use of polyurethane for structural and infrastructural engineering applications : A state-of-the-art review,” vol. 190, pp. 995–1014, 2018.

[13] P. Banerjee and P. Sallomi, “3D opportunity for technology, media, and telecommunications. Additive manufacturing explores new terrain,” 2015.

[14] S. W. Kwok *et al.*, “Electrically conductive filament for 3D-printed circuits and sensors,” *Appl. Mater. Today*, vol. 9, pp. 167–175, Dec. 2017.

[15] K. Angel, H. H. Tsang, S. S. Bedair, G. L. Smith, and N. Lazarus, “Selective electroplating of 3D printed parts,” vol. 20, no. November 2017, pp. 164–172, 2018.

[16] M. R. N. Esfahani *et al.*, “Hybrid Additive Manufacture of Conformal Antennas,” in *2018 IEEE MTT-S International Microwave Workshop Series on Advanced Materials and Processes for RF and THz Applications (IMWS-AMP)*, pp. 1–3, 2018.

[17] D. Strong, M. Kay, B. Conner, T. Wake, and G. Manogharan, “Hybrid manufacturing – integrating traditional manufacturers with additive manufacturing (AM) supply chain,” vol. 21, pp. 159–173, 2018.

[18] A. Equbal, A. Equbal, and A. K. Sood, “Metallization on FDM Processed Parts Using Electroless Procedure,” *Procedia Mater. Sci.*, vol. 6, pp. 1197–1206, Jan. 2014.

[19] N. Saleh, N. Hopkinson, R. J. M. Hague, and S. Wise, “Effects of electroplating on the mechanical properties of stereolithography and laser sintered parts,” *Rapid Prototyp. J.*, vol. 10, no. 5, pp. 305–315, Dec. 2004.

[20] A. Ryspayeva *et al.*, “Selective Electroless Copper Deposition by Using Photolithographic Polymer/Ag Nanocomposite,” *IEEE Trans. Electron Devices*, vol. 66, no. 4, pp. 1–6, 2019.

[21] J. Yang, J. H. Cho, and M. J. Yoo, “Selective metallization on copper aluminate composite via laser direct structuring technology,” *Compos. Part B Eng.*, vol. 110, pp. 361–367, Feb. 2017.

[22] K. Ratautas *et al.*, “Laser-induced selective metallization of polypropylene doped with multiwall carbon nanotubes,” *Appl. Surf. Sci.*, vol. 412, pp. 319–326, Aug. 2017.

[23] M. Gedvilas *et al.*, “Colour-Difference Measurement Method for Evaluation of Quality of Electrolessly Deposited Copper on Polymer after Laser-Induced Selective Activation,” *Sci. Rep.*, vol. 6, no. 22963, pp. 1–8, 2016.

[24] J. Marques-Hueso *et al.*, “A Rapid Photopatterning Method for Selective Plating of 2D and 3D Microcircuitry on Polyetherimide,” *Adv. Funct. Mater.*, vol. 28, no. 6, pp. 1–8, 2018.

[25] “Rubber, vulcanized or thermoplastic — Determination of

This work is licensed under a Creative Commons Attribution 4.0 License. For more information, see https://creativecommons.org/licenses/by/4.0/.

This article has been accepted for publication in a future issue of this journal, but has not been fully edited. Content may change prior to final publication. Citation information: DOI 10.1109/ACCESS.2019.2931594, IEEE Access

indentation hardness — Part 1: Durometer method (Shore hardness),” Geneva, 2004.

[26] T. D. A. Jones *et al.*, “Direct metallisation of polyetherimide substrates by activation with different metals,” *Surf. Coat. Technol.*, vol. 360, pp. 285–296, 2019.

[27] “Ipc-tm-650 test methods manual 1,” 2215 Sanders Road Northbrook, IL 60062-6135, 2004.

[28] M. D. Manrique-Juárez, A. L. Martínez-Hernández, O. F. Olea-Mejía, J. Flores-Estrada, J. L. Rivera-Armenta, and C. Velasco-Santos, “Polyurethane-Keratin Membranes: Structural Changes by Isocyanate and pH, and the Repercussion on Cr(VI) Removal,” *Int. J. Polym. Sci.*, vol. 2013, pp. 1–12, 2013.

[29] “Recreus FILAFLEX ORIGINAL 82A MSDS,” Alicante, 2019.

[30] K. A. Chaffin, X. Chen, L. Mcnamara, F. S. Bates, and M. A. Hillmyer, “Polyether Urethane Hydrolytic Stability after Exposure to Deoxygenated Water,” *Macromolecules*, vol. 47, no. 15, pp. 5220–5226, 2014.

[31] P. Y. Le Gac, D. Choqueuse, and D. Melot, “Description and modeling of polyurethane hydrolysis used as thermal insulation in oil offshore conditions,” *Polym. Test.*, vol. 32, no. 8, pp. 1588–1593, 2013.

[32] J. V Cauich-Rodríguez, L. H. Chan-Chan, F. Hernandez-Sánchez, and J. M. Cervantes-Uc, “Degradation of Polyurethanes for Cardiovascular Applications,” 2013.

[33] K. P. C. Vollhardt and N. E. Schore, *Organic Chemistry*, 2nd edition. W. H. Freeman and Company, 1994.

[34] George Socrates, *Infrared and Raman Characteristic Group Frequencies*, Third Edit. JOHN WILEY & SONS, LTD, 2001.

[35] E. Baştürk, S. Madakbaş, M. V. Kahraman, E. Baştürk, S. Madakbaş, and M. V. Kahraman, “Improved Thermal Stability and Wettability Behavior of Thermoplastic Polyurethane / Barium Metaborate Composites,” *Mater. Res.*, vol. 19, no. 2, pp. 434–439, Feb. 2016.

[36] C. Sien Wong and K. Haji Badri, “Chemical Analyses of Palm Kernel Oil-Based Polyurethane Prepolymer,” *Mater. Sci. Appl.*, vol. 3, pp. 78–86, 2012.

[37] A. Asefnejad, “Manufacturing of biodegradable polyurethane scaffolds based on polycaprolactone using a phase separation method : physical properties and in vitro assay,” *Int. J. Nanomedicine*, vol. 6, pp. 2375–2384, 2011.

[38] Z. Shah, L. Krumholz, D. F. Aktas, F. Hasan, M. Khattak, and A. A. Shah, “Degradation of polyester polyurethane by a newly isolated soil bacterium, Bacillus subtilis strain MZA-75,” *Biodegradation*, vol. 24, no. 6, pp. 865–877, 2013.

[39] A. L. Gonzalez, C. Noguez, J. Beranek, and A. S. Barnard, “Size, Shape, Stability, and Color of Plasmonic Silver Nanoparticles,” *J. Phys. Chem.*, vol. 118, p. 9128−9136, 2014.

[40] A. Ryspayeva *et al.*, “PEI/Ag as an optical gas nano-sensor for intelligent food packaging,” in *2018 IEEE Int. Conf. Nanotechnolog.*, 2018.

[41] J. Marques-Hueso, J. A. S. Morton, X. Wang, E. Bertran-Serra, and M. P. Y. Desmulliez, “Photolithographic nanoseeding method for selective synthesis of metal-catalysed nanostructures,” *Nanotechnology*, vol. 30, no. 1, p. 15302, Jan. 2019.

[42] M. Paunovic, “Electroless Deposition of Copper,” *Mod. Electroplat. Fifth Ed.*, vol. 1, pp. 433–446, 2010.

[43] J. E. A. M. van Meerakker and E. Scholtens, “Side Reactions in Electroless Copper Solutions with Formaldehyde as Reducing Agent,” *Berichte der Bunsengesellschaft für Phys. Chemie*, vol. 93, no. 7, pp. 786–791, Jul. 1989.

[44] T. Ogura and M. Malcomson, “Mechanism of copper deposition in electroless plating,” *Langmuir*, vol. 1, no. 7, pp. 1709–1710, 1990.

[45] S. Nakahara and Y. Okinaka, “The hydrogen effect in copper,” *Mater. Sci. Eng. A*, vol. 101, pp. 227–230, May 1988.

[46] S. Nakahara, “Microscopic mechanism of the hydrogen effect on the ductility of electroless copper,” *Acta Metall.*, vol. 36, no. 7, pp. 1669–1681, Jul. 1988.

[47] W. Sha, X. Wu, and K. G. Keong, *Electroless Copper and Nickel-Phosphorus Plating: Processing, Characterisation and Modelling*. Woodhead Pub, 2011.

This work is licensed under a Creative Commons Attribution 4.0 License. For more information, see https://creativecommons.org/licenses/by/4.0/.